

See discussions, stats, and author profiles for this publication at: <https://www.researchgate.net/publication/215537688>

# Rheological properties of carboxymethyl cellulose (CMC) solutions. Colloid Polym Sci

ARTICLE *in* COLLOID AND POLYMER SCIENCE · SEPTEMBER 2008

Impact Factor: 1.87 · DOI: 10.1007/s00396-008-1882-2

---

CITATIONS

62

---

READS

1,047

## 2 AUTHORS:



[Adel Benchabane](#)

Université de Biskra

54 PUBLICATIONS 301 CITATIONS

[SEE PROFILE](#)



[Bekkour Karim](#)

University of Strasbourg

49 PUBLICATIONS 250 CITATIONS

[SEE PROFILE](#)

# Rheological properties of carboxymethyl cellulose (CMC) solutions

Adel Benchabane · Karim Bekkour

Received: 29 February 2008 / Revised: 24 April 2008 / Accepted: 30 April 2008 / Published online: 31 May 2008  
© Springer-Verlag 2008

**Abstract** In this study, we investigated the way of predicting two critical concentrations of sodium carboxymethyl cellulose (CMC) solutions using simple experimental procedures with a rotational rheometer. It was found that, above a critical shear rate, all CMC solutions (0.2 to 7 wt. %) exhibit shear-thinning behavior and the flow curves could be described by the Cross model. A first critical CMC concentration  $c^*$ , transition to semidilute network solution, was determined using the following methods (1) study of the flow curve shapes, (2) Cross model parameters, (3) plot of the specific viscosity vs the overlap parameter, and (4) empirical structure-properties relationships. Furthermore, both creep and frequency-sweep measurements showed that the solutions behaved as viscoelastic materials above a second critical CMC concentration  $c^{**}$  (transition to concentrated solution). The characterization of CMC solutions was completed with a time-dependent viscosity study that showed that the CMC solutions exhibited strong thixotropic behavior, especially at the highest CMC concentrations.

**Keywords** Shear-thinning · Cross model · Critical concentration · Viscoelasticity · Thixotropy

## Introduction

The addition of organic additives to clay suspensions is of great industrial interest because of their capacity to modify their colloidal and rheological properties. For example, water-based drilling fluids have numerous roles such as stabilizing the borehole by forming a cake, cleaning the hole by evacuating the cuttings, and cooling and lubricating the string and the bit, and additives, generally polymers, are sought to enable clay suspension to fulfill these functions [1]. Precisely, in such materials, where bentonite is a major component, carboxymethyl cellulose (CMC) is appropriate for increasing the viscosity, controlling the mud fluid loss, and maintaining adequate flow properties at high temperature, salinity, and pressure. CMC is a cellulose derivative with a variety of different end-uses in numerous industries. In drilling fluids, it is appropriate for stabilizing and plastering the clay suspension, increasing the viscosity, controlling the mud losses, and maintaining adequate flow properties at in situ conditions. In cosmetic and pharmaceutical applications, CMC is used in various products, creams, lotions, and toothpaste formulation where its good binding, thickening, and stabilizing properties are utilized. Furthermore, due to its polymeric structure that acts as film-forming agent, it is also used to improve moisturizing effects. Among numerous other applications, CMC is used in textile industry as a coating agent, in resin emulsion paints, adhesive and printing inks, and in coating colors for the pulp and paper industry, to cite just a few. Although other gums with comparable properties are available on the market, CMC is frequently the product of choice due to its

---

A. Benchabane · K. Bekkour (✉)  
Institut de Mécanique des Fluides et des Solides,  
UMR CNRS-ULP 7507,  
2, rue Boussingault,  
67000 Strasbourg, France  
e-mail: karim.bekkour@imfs.u-strasbg.fr

### Present address:

A. Benchabane  
Département de Génie Mécanique,  
Université Mohamed Khider Biskra,  
B.P. 145 R.P.,  
07000 Biskra, Algeria

favorable price-to-performance ratio. CMC is also used in paper, ceramic, and food industries [2]. Surprisingly, although widely utilized as additive in clay suspensions, very few papers were published on the exclusive influence of CMC on the rheological properties of clay dispersions [2–6].

The rheological properties of CMC solutions are much more documented [7–10] even though many aspects of these solutions are still in the focus of polymer research and the subject of a great deal of experimental and theoretical work [11–13]. Ghannam and Esmail [7] have investigated the rheological properties of CMC solutions in the concentration range 1–5% and have reported nearly Newtonian behavior at the lowest concentration and pseudoplastic, thixotropic, and viscoelastic responses at the higher-end concentrations. Nevertheless, they did not report the molecular weight of the polymer used, which is, of course inconvenient when the comparison of the different experimental results is needed. Edali et al. [8] have investigated the rheological behavior of CMC solutions at higher concentrations and have confirmed both non-Newtonian and viscoelastic properties that have been found to be much more pronounced. Kulicke et al. [9] have established relationships between the molecular structure of CMC and the rheological properties of the aqueous solutions over the CMC concentration range 0.5–3%. They reported that the molar mass and the polymer concentration are the governing parameters, whereas the degree of substitution (DS) has only a little influence affecting primarily the solubility. Clasen and Kulicke [10] in their review paper have investigated the pseudoplastic flow behavior, the viscoelastic, and the rheo-optical properties of various water-soluble cellulosic derivatives and summarized the correlations between the viscosity data and the molecular structure parameters.

The scope of the present paper is to provide a complete and comprehensive rheological investigation of CMC solutions, in particular investigating the presence of a critical shear rate at which a change in the behavior of the flow curves occurs, and the relationship between the critical CMC concentrations and the rheological behavior of the polymer solutions. This will allow to further extend the experimental investigation of CMC–bentonite mixtures previously studied by the authors [3] in order to better understand the physical phenomena responsible for the changes induced by the addition of an anionic polymer on the rheological and colloidal properties of bentonite suspensions. To do so, the rheological properties of CMC solutions at different concentrations (0.2% to 7%) are studied. In a forthcoming publication, the effect of the addition of CMC to bentonite dispersions will be investigated.

## Materials and methods

### Materials and sample preparation

The CMC, with a nominal molecular weight of 700,000 g mol<sup>-1</sup> and a DS of 0.65–0.85, used in the present work was supplied from Sigma-Aldrich. Preliminary tests showed that the preparation of CMC solutions requires a minimum time to fully dissolve the CMC powder. This time depends on the polymer concentration and the temperature. Consequently, aqueous solutions of CMC were prepared by dissolving the appropriate amount of CMC in distilled water at room temperature. Exceptionally, the high CMC concentration solutions, with weight concentrations ranging from 4% to 7%, were prepared by using water heated at 50 °C. In addition, sufficient time ( $\leq 48$  h) of gentle stirring was allowed to achieve complete hydration and avoiding air bubbles formation.

### Experimental methods

All the rheological measurements were performed on a controlled stress rheometer (AR2000, TA Instruments) equipped with a cone-and-plate geometry (diameter 40 mm; angle 0.034 radian) at controlled temperature of 20.0 $\pm$ 0.1 °C. Since the domain structure of CMC solutions is quite sensitive to shear deformation history, the solutions were gently stirred for 1 h; afterwards, the samples were carefully loaded to the measuring plate of the rheometer using a spatula and then the measuring cone was lowered at a very slow speed, in order to prevent the disruption of the solution structure. The samples were then left to rest for 10 min prior to the measurements. A solvent trap geometry was used to prevent sample evaporation via saturation of the enclosed volume.

The flow curves were obtained by applying an increasing shear stress ramp at a constant stress rate of 0.03 Pa s<sup>-1</sup>. However, for the low CMC concentrations (<1%), the stress rate was set at a lower value (less than 0.03 Pa s<sup>-1</sup>) in order to obtain more detailed flow curves in the range of low shear rates. The thixotropic behavior was investigated by evaluating the hysteresis loop areas obtained through a three-step experiment (upward curve, plateau, and downward curve). The linear viscoelastic properties of the aqueous solutions of CMC were studied firstly in terms of transient properties using creep experiments. A creep curve is obtained by applying at time  $t_0$  a shear stress,  $\tau=0.08$  Pa, held constant, and measuring the time evolution of the resultant deformation followed by a strain recovery curve obtained after removal of the constant stress at  $T=300$  s. Secondly, the storage  $G'(\omega)$  and loss  $G''(\omega)$  moduli were measured at frequencies ranging from 0.01 to 10 Hz and,

by applying a chosen stress value, allowing measurements within the linear viscoelastic region.

## Results and discussion

### Shear flow measurements

Figure 1a shows the flow curves of the CMC solutions at different concentrations plotted over a log–log scale that covers nearly six decades of shear rate. It can be clearly seen that the apparent viscosity increases with increasing concentrations. This rise in the apparent viscosity is due to the increase in the intermolecular interactions between the CMC molecules. As previously reported in the literature [7, 8], at all the concentrations investigated here, there was no evidence of a yield stress. Furthermore, it is obvious that these curves are nonlinear, which indicates that the power law model of Ostwald-de Waele, generally utilized to fit flow curves of CMC solutions, is not suitable. It must be underlined here that this conclusion differs from the results generally published by other authors. Ghannam and Esmail [7], for CMC solutions from 1% to 5%, and Edali et al. [8], for CMC solutions from 5% to 8%, among others, reported a power law behavior over a shear rate domain of 0–1,000  $\text{s}^{-1}$ . An attentive analysis of their results reveals that the linear fit, in the log–log scale, of shear stress–shear rate curves, is only a crude approximation of the experimental data.

Figure 1b plots the same data as in Fig. 1a in terms of viscosity as a function of shear rate. Depending on the CMC concentration, different flow behaviors are observed. The lowest concentrations (0.2%, 0.4%, and 0.8%) exhibit two shear-thinning behaviors over two ranges of shear rates separated by a plateau value at medium shear rate. Attention should be drawn to the sigmoid curves with a point of inflection that corresponds to change in the rheological behavior. At higher CMC concentrations, above 1%, the viscosity curves are quite different, i.e., an initial shear-thickening behavior is observed, where the apparent viscosity increases with increasing shear rate, followed at a given shear rate by a shear-thinning behavior. Similar observations have been made by other authors. Liu et al. [14] reported Newtonian or shear-thinning behavior of polymer solutions at low shear rates and shear-thickening behavior when the shear rate is increased above a critical value. Moreover, when the shear rate is further increased, shear-thinning behavior is observed. In practice, this means that the flow encounters less resistance at higher shear rates. It is admitted that this shear-thinning behavior is caused by the disentanglement of the polymer coils in solution or increased orientation of the polymer coils in the direction of

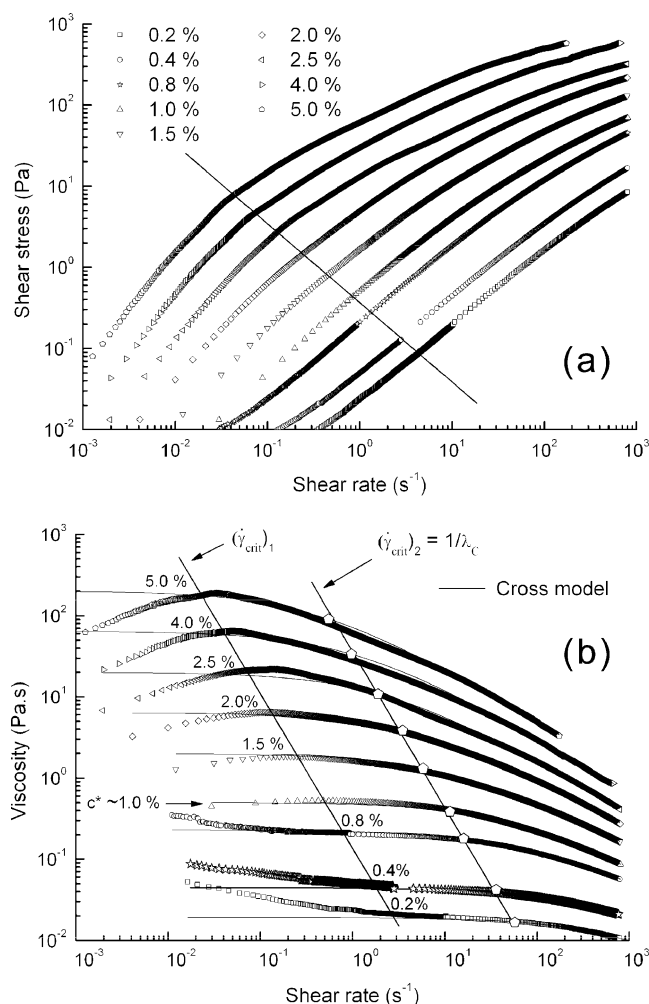


**Fig. 1** a Flow behavior curves of CMC solutions at different concentrations. b Viscosity as a function of shear rate for CMC solutions at different concentrations. Solid lines are obtained using the Cross model with  $\dot{\gamma}_{c1}$  and  $\dot{\gamma}_{c2}$  the first and second critical shear rate

the flow [10, 15]. The shear-thickening behavior observed below the critical shear rate (for CMC concentrations above the critical concentration of 1%) was also investigated by others in the neighborhood of the critical concentration, usually mentioned in the literature as the overlap concentration [14]. The mechanism for this shear-thickening behavior is still a matter of discussion, and various explanations have been proposed to account for the shear-thickening behavior of polymer solutions. Liu et al. [14] reported that one of the most accepted interpretations is the “flow-induced formation of macromolecular associations”. We also think that the observed shear thickening could be interpreted as the result of a stiffer inner structure due to the formation of entanglements of polymer coils and the increase in the intermolecular interactions, as the shear rate rises.

Thus, from the shapes of the flow curves depicted on Fig. 1b, the CMC concentration of 1% seems to be a critical

one, i.e., the overlap concentration. As up to this concentration, the solutions experience a rheological behavior quiet different from those of the higher concentrations, i.e., a Newtonian plateau at low shear rates which corresponds to that of the zero shear viscosity and transition to the shear-thinning region at higher shear rates (see Fig. 1b). Moreover, a critical shear rate  $\dot{\gamma}_{c1}$  at which the onset of the Newtonian plateau is evaluated is also shown in Fig. 1b. This critical shear rate shifts towards lower values of shear rate as the CMC concentration increases. Hence, over the range of shear rates  $\dot{\gamma}_{c1} < \dot{\gamma} < 1,000\text{s}^{-1}$ , only two distinct ranges of Newtonian and non-Newtonian shear-thinning behaviors were recorded for all CMC concentrations. Above the first critical shear rate  $\dot{\gamma}_{c1}$ , the data were seen to be well represented by the well-known Cross model for all concentrations (Fig. 1b):

$$\frac{\mu - \mu_{\infty}}{\mu_0 - \mu_{\infty}} = \frac{1}{1 + (\lambda_c \cdot \dot{\gamma})^n} \quad (1)$$

where  $\mu$  is the viscosity at any particular shear rate  $\dot{\gamma}$ ,  $\mu_0$  and  $\mu_{\infty}$  are asymptotic values of viscosity at zero and infinite shear rates, respectively,  $\lambda_c$  is a time constant with the dimensions of time and  $n$  is a dimensionless rate constant indicating the degree of dependence of viscosity on shear rate in the shear-thinning region. A value of 0 for  $n$  indicates Newtonian behavior, with  $n$  tending to unity for increasing shear-thinning behavior. The reciprocal of the time constant,  $1/\lambda_c$ , corresponds to a critical shear rate that provides a useful indicator of the onset shear rate for shear thinning. Figure 1b shows the application of the Cross model to the experimental data in the range  $\dot{\gamma} > \dot{\gamma}_{c1}$  and the accompanying results are listed in Table 1. Zero and infinite shear rate viscosities  $\mu_0$  and  $\mu_{\infty}$ , and the characteristic time  $\lambda_c$  were found to increase with increasing CMC concentration from 0.2% to 6%, whereas the rate index  $n$  remains constant. Figure 1b also depicts the second critical shear rate  $\dot{\gamma}_{c2} = 1/\lambda_c$  for the different

CMC concentrations studied. It is worth noticing that the critical shear rate viscosity data fit very well with a power law function of the form:

$$\mu = 33.5 \cdot (\dot{\gamma}_{c2})^{-1.9} \quad (2)$$

Furthermore, for CMC concentrations  $\geq 2.5\%$  (which seems to correspond to a second critical concentration) and over the range of shear rates  $\dot{\gamma}_{c1} < \dot{\gamma} < 1,000\text{s}^{-1}$ , we found that the steady shear viscosity data of the CMC solutions studied coincide on the same master curve when plotting  $(\mu - \mu_{\infty})/(\mu_0 - \mu_{\infty})$  as a function of the dimensionless shear rate  $(\lambda_c \dot{\gamma})^n$ .

In order to understand the physical significance of above-observed critical concentrations, 1.0% and 2.5%, we first refer to Graessley's [16] work. This author showed that for a complete description of polymer fluids over the whole concentration range, i.e., from volume fraction  $\phi \rightarrow 0$  to  $\phi = 1$ , in a thermodynamically good solvent, five distinct states of solution must be taken into account. These five states of solution are: (1) ideally dilute particle solution, (2) semidilute particle solution, (3) semidilute network solution, (4) concentrated particle solution, and (5) concentrated network solution [16, 17]. Usually, the critical concentration delimitating the semidiluted nonentangled solution and the semidiluted entangled network solution can be determined by the overlap parameter,  $c.[\mu]$ , plotted as a function of the specific viscosity,  $\mu_{sp}$ , defined as:

$$\mu_{sp} = \frac{\mu_0 - \mu_s}{\mu_s} \quad (3)$$

and:

$$[\mu] = \lim_{\substack{c \rightarrow 0 \\ \dot{\gamma} \rightarrow 0}} \left( \frac{\mu_{sp}}{c} \right) \quad (4)$$

where  $c$  is the CMC concentration,  $[\mu]$ ;  $\mu_s$  and  $\mu_0$  are the intrinsic, the solvent and the zero shear rate viscosities, respectively [10, 17].

Figure 2a plots the overlap parameter  $c.[\mu]$  as a function of the specific viscosity  $\mu_{sp}$ . The slope change at a given value of  $c.[\mu]$  ( $c.[\mu] \sim 23$ ) suggests the presence of a critical CMC concentration, corresponding to the critical concentration  $c^* \sim 1\%$  reported above (see Fig. 1b), at which occurs a microstructure evolution from a semidiluted nonentangled solution to a semidiluted entangled network. A confirmation of this assumption is found in the review article of Clasen and Kulicke [10]. These authors have demonstrated that for semidiluted solutions of cellulosic derivatives, the viscosity of the Newtonian flow range,  $\mu_0$ , can be described from a master curve with the aid of an empirical structure–

**Table 1** Cross model constants of CMC solutions.

CMC (%)	$\lambda_c$ (s)	$n$ (-)	$\mu_0$ (Pa s)	$\mu_{\infty}$ (Pa s)
0.2	0.010	0.67	0.019	0.001
0.4	0.016	0.65	0.045	0.001
0.8	0.060	0.60	0.230	0.002
1.0	0.088	0.61	0.530	0.003
1.5	0.172	0.64	1.970	0.020
2.0	0.287	0.66	6.355	0.024
2.5	0.530	0.69	21	0.038
3.0	0.865	0.69	48	0.040
4.0	1.026	0.68	70	0.040
5.0	1.804	0.67	200	0.045
6.0	3.459	0.67	700	0.060

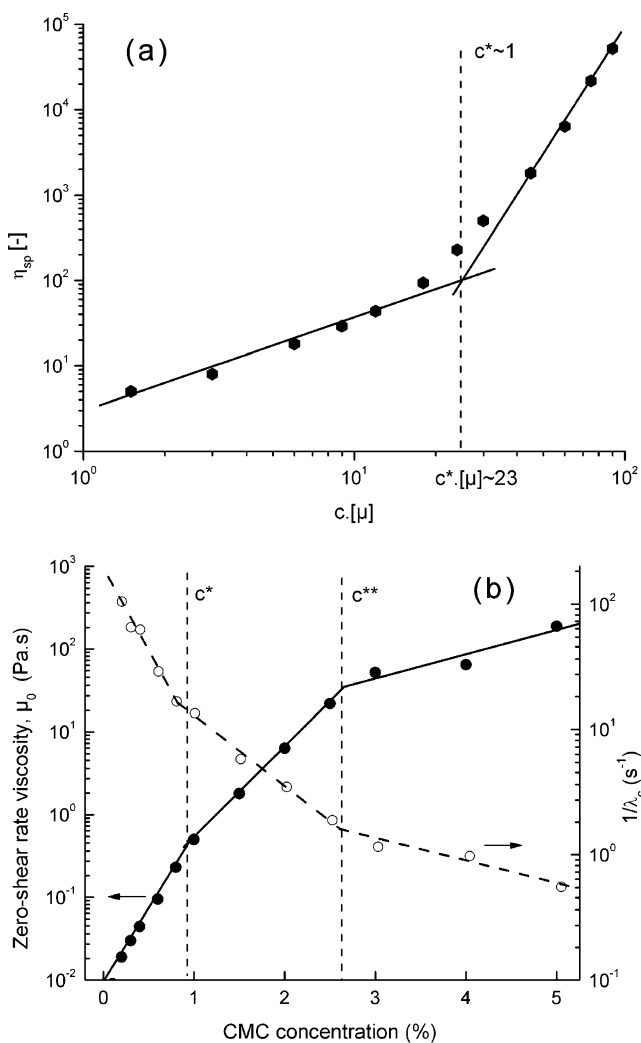


**Fig. 2** **a** Overlap parameter,  $c.[\mu]$ , as a function of specific viscosity,  $\mu_{sp}$ , at different concentrations of CMC solutions. **b** The reciprocal of the time constant,  $1/\lambda_c$ , and the zero shear rate viscosity,  $\mu_0$ , as a function of CMC concentration

property relationship ( $\mu_0, M_w, c$ ), given by the following expression:

$$\mu_0 = 0.891 + 7.82 \cdot 10^{-3} \cdot cM_w^{0.93} + 1.77 \cdot 10^{-5} \cdot c^2M_w^{1.86} + 4.22 \cdot 10^{-12} \cdot c^{4.09}M_w^{3.80} \quad (5)$$

where  $\mu_0$  is the zero shear rate viscosity,  $c$  is the CMC concentration, and  $M_w$  is the molecular weight. A reasonable value for the critical overlap parameter  $c^*.[\mu]$  was proposed [10], i.e.,  $c^*.[\mu]=23$ . This value leads, by the use of Eq. 5, to a critical concentration value of 0.9%, which is very close to the value of 1% obtained by our rheological experiments (see Fig. 2a).

Figure 2b shows the evolution of the zero shear rate viscosity and the reciprocal time constant,  $1/\lambda_c$ , as a function of the CMC concentration. It is worth noticing the abrupt slope change in both zero viscosity  $\mu_0$  and  $1/\lambda_c$

vs CMC weight concentration curves at same CMC concentrations, around 1% and 2.5%. This change could be clearly related to the inner structure of CMC solutions and corresponds respectively to (1) the critical overlap concentration  $c^*$  as explained above and (2) to the second critical concentration,  $c^{**}$ , which will be confirmed below by the viscoelastic experiments.

### Thixotropy

CMC solutions are known to be strongly time-dependent materials, which mean that they exhibit a viscosity–time relationship, where the viscosity decreases with the shearing time [6–8]. The time-dependent behavior of the viscosity is related to changes occurring in the inner structure of the fluid due to particle interaction forces like the Van de Waals forces, which are responsible for the formation of flocs and aggregates. These forces act at microscopic scale between dispersed species in the material and, above a certain particle volume fraction, may lead to the formation of a rigid continuous particle network, which can withstand the flow [18]. In general, two types of experiments can be conducted for the investigation of the thixotropic properties of the materials [18, 19]: (1) the equilibrium flow curves for which the shear stress (or shear rate, i.e., with the controlled shear rate rheometer) was held at a constant level and the shear rate (or shear stress) was recorded as a function of time until the equilibrium value was reached and (2) the shearing cycles consisted of successive increasing and decreasing shear stress (hysteresis loops). Many authors have investigated the thixotropic properties of CMC solutions [6–8], using hysteresis experiments. This approach involves the determination of the area enclosed between up curves and down curves obtained with loading and unloading measurements, respectively. The area of hysteresis loops may be considered as an estimation of the degree of thixotropy, and it is generally admitted that the greater the hysteresis area, the stronger the thixotropic properties. The tests carried out in the present study showed that the CMC solutions exhibited strong thixotropic properties. A typical experimental protocol consisted of a three-step operation. An increasing shear stress ramp at a constant stress rate of  $0.03 \text{ Pa s}^{-1}$  from zero to a prefixed maximum value (upward flow curve), followed by a plateau at the maximum shear stress for 30 min (peak hold) and, thereafter, the ramp was reversed to measure downward flow curve for 10 min. The upward and downward flow curves should be the same for a time-independent liquid and should not superpose in the case of a time-dependent liquid. As mentioned above, most authors, when evaluating the thixotropy of materials, take into account the area of hysteresis loops measured by loading–unloading experiments. This area has the dimensions of power per unit volume ( $\text{Pa s}^{-1}$  or  $\text{ML}^2\text{T}^{-3}/\text{L}^3 = \text{ML}^{-1}\text{T}^{-3}$ , where  $M$  represents

the dimension of a mass,  $L$ , length, and  $T$ , time) and corresponds to the power necessary to break down the thixotropic structure of a given volume of solution. We propose to evaluate the degree of thixotropy of CMC solutions by using a slightly different method. We define a dimensionless thixotropic index  $\alpha$  by reporting the area of the thixotropic loop to the area under the upward flow curve:

$$\alpha = 100 \cdot [(U - D)/U] \quad (6)$$

In Eq. 6,  $U$  and  $D$  designate the areas under the up curve and the down curve, respectively. Figure 3 shows the variation of the thixotropic index  $\alpha$  as a function of CMC concentration. It may be seen that the greater the polymer concentration, the stronger the time dependence behavior. Several authors [20–23] related this observation to the shear-thinning behavior of CMC solutions (Fig. 1) and suggested that the rate of the disentanglement of the macromolecules by shearing is higher than that of re-entanglement [22, 23]. Consequently, the thixotropic behavior of CMC solutions can be attributed to these disentanglement–entanglement processes and to the alignment of the polymer chains along the direction of shear [20, 21].

#### Viscoelastic properties of CMC solutions

Dynamic and creep rheometry are efficient tools for investigating the properties of polymer solutions under conditions close to the at-rest state, allowing to investigate the viscoelastic properties without the disruption of the internal structure of the system. Thus, the test simply flexes organized structures as gel networks but does not disrupt them. Furthermore, the data obtained from the dynamic and creep measurements could be interpreted in the framework of the linear viscoelastic theory.

The experiments consisted first of creep tests and, consequently, the elastic properties were defined by correlating the results with the well-known generalized viscoelas-

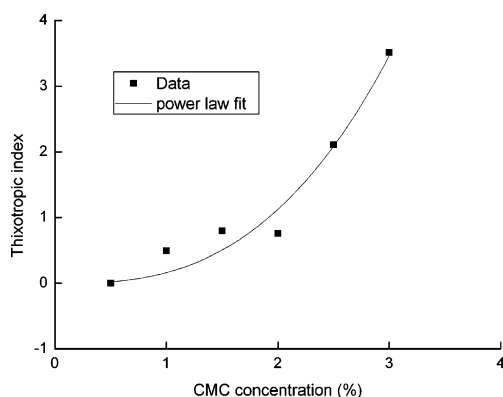


**Fig. 3** Evolution of the thixotropic index with the CMC concentration. Solid line is a power law fit to data

tic model of Kelvin–Voigt that can be physically described by assemblies of dashpots and springs: a Maxwell unit (Newtonian dashpot in series with purely elastic spring) in series with one or more Kelvin–Voigt units (dashpots in parallel with springs). The creep compliance [or deformation per unit stress,  $f(t) = \gamma(t)/\tau$ ] is then given by:

$$f(t) = J_0 + \sum_{i=1}^n J_i \left(1 - e^{-t/\theta_i}\right) + t/\mu_N \quad (7)$$

whereas the recovery strain is given by:

$$\gamma_r = \sum_i^N J_i (e^{T/\theta_i} - 1) + T/\mu_N \quad (8)$$

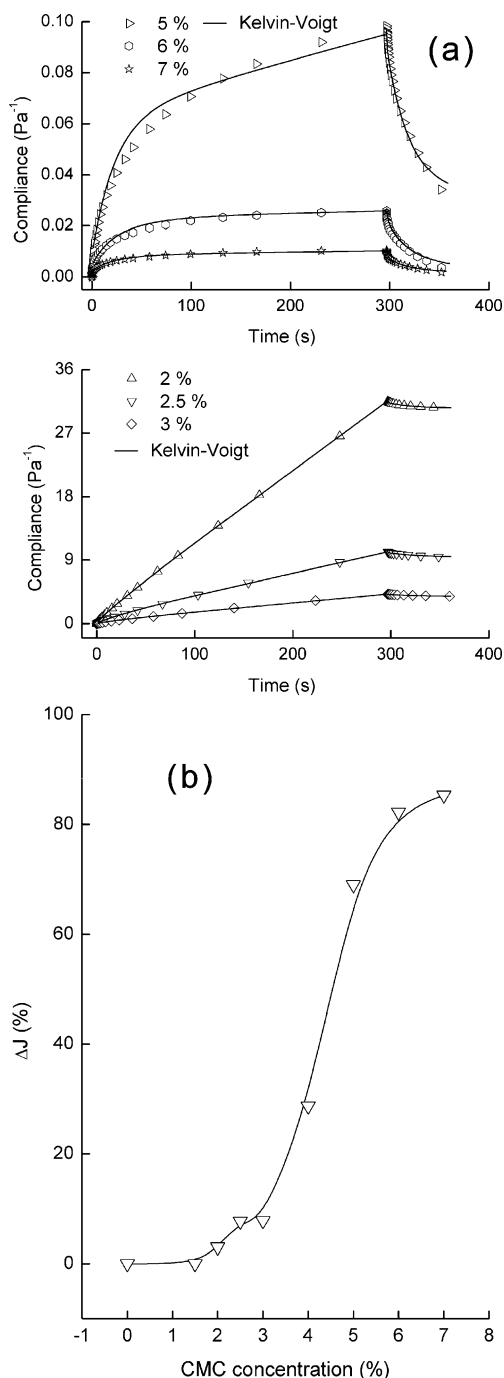
where  $f(t)$  is the overall creep compliance at the time  $t$ ,  $J_0$  is the purely elastic contribution (or the instantaneous elastic compliance) and  $\mu_N$  is the purely viscous contribution, represented by the dashpot of the Maxwell model, i.e., the uncoupled or residual steady-state viscosity obtained from the creep curve at long times when the compliance curve is linear. The set  $(J_i, \theta_i, i=1 \dots N)$  is the discrete distribution (or discrete spectrum) of retardation times  $\theta_i$  where  $J_i$  is the contribution to retarded elastic compliance of the  $i^{\text{th}}$  component with a retardation time  $\theta_i = J_i \mu_i$  and a viscosity  $\mu_i$ . The viscoelastic parameters were derived from the creep compliance–time curves by the use of the well-known method initially developed by Inokuchi [24, 25].

Figure 4a shows the viscoelastic properties of the CMC solutions at different concentrations in terms of creep recovery response. It may be observed that for concentrations below 2.5%, the compliance curves are typical of viscous materials without elasticity. However, for CMC concentrations above 2.5%, an elastic behavior is observed. For all CMC concentrations, a decrease of the elastic compliance (or an increase of the elastic modulus  $E=1/J$ ), with the increase in concentration is observed. This indicates that the creep deformation decreases with increasing the polymer concentration and the time necessary to reach a constant deformation during recovery, after removal of the shear stress decreases. This is characteristic of systems whose links in the inner structure strengthen when the concentration is increased, in agreement with the shear flow experiments results (see Fig. 1a). This effect can be quantified by calculating the recovery attained by the systems upon removing the stress [26]:

$$\Delta J = 100 \cdot \frac{J(300) - J(360)}{J(300)} \quad (9)$$

For low-range concentrations of CMC solutions, very low values of the elastic recovery index  $\Delta J$  are obtained, which is a characteristic of the behavior of a viscous fluid. For the highest CMC concentrations,  $\Delta J$  was found to be

close to 90%, i.e., elastic solid-like behavior. Figure 4b illustrates the variation of the elastic recovery index  $\Delta J$  as a function of CMC concentration. A dramatic increase of the elastic recovery index  $\Delta J$ , at a CMC concentration close to 2.5%, is observed. This confirms the results obtained in the shear flow experiments (see Fig. 2b), which did show a critical concentration  $c^{**}=2.5\%$ .



**Fig. 4** **a** Creep recovery curves of CMC solutions at different concentrations. **b** Variation of the elastic recovery index  $\Delta J$  as a function of CMC concentration

In addition to the transient properties discussed previously, oscillatory tests were carried out. The elastic modulus  $G'$  and the viscous modulus  $G''$  as functions of frequency are reported in Fig. 5. The measurements were performed by applying a small stress to ensure to remain within the linear region. It is very interesting to observe how the relative  $G'$  and  $G''$  position changes with changing the CMC concentration. For clarity, all the collected data are not reported in these figures although they show similar trend. From these results, the following observations could be made: (1) The lowest CMC concentration solutions exhibit  $G''$  values higher than  $G'$  values. This means that, at low CMC concentrations, the viscous properties are dominant compared to the elastic ones. This is a confirmation of the creep experiments results which showed that low CMC concentration solutions are dominantly viscous-like materials (see Fig. 4a); (2) At CMC concentrations close to 2.5%, a

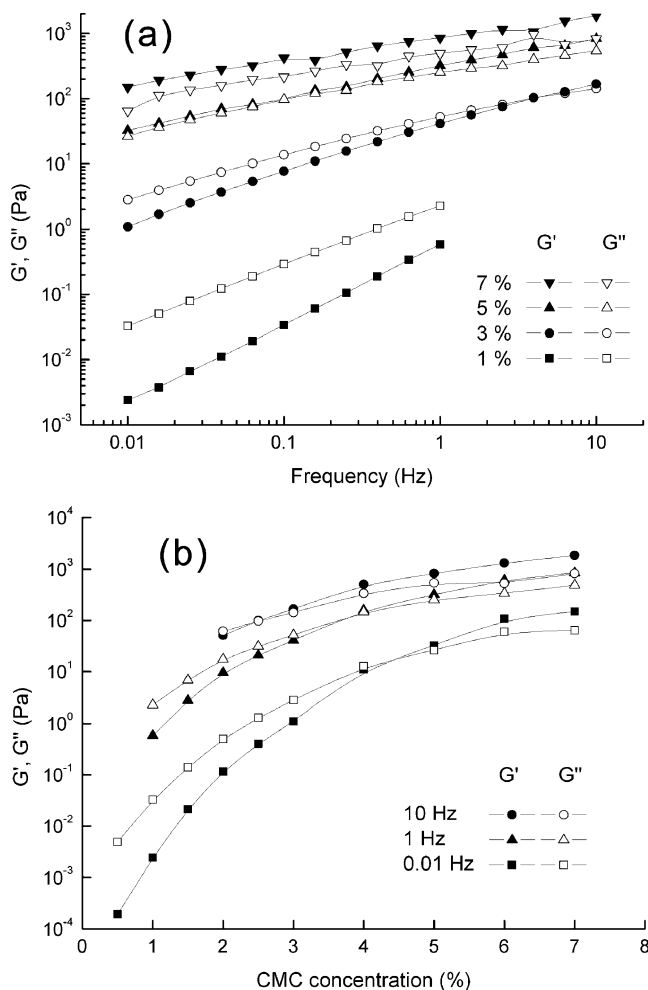


**Fig. 5** **a** Variation of loss and storage moduli as a function of frequency for different CMC concentrations. **b** Variation of loss and storage moduli at different frequencies as a function of CMC concentration

transition could be observed at the highest frequencies, where the storage modulus  $G'$  was found to be higher than the loss modulus  $G''$  for CMC concentrations,  $c > c^{**} = 2.5\%$  (see Figs. 2 and 4). These observations are well confirmed by Fig. 5b where  $G'$  and  $G''$  as a function of the CMC concentration at 0.01, 1, and 10 Hz are reported. Finally, based on the shear flow experiments, this behavior could be related to the formation of a three-dimensional network. At the highest polymer concentrations, the local polymer–polymer interactions (entanglements) are the main factor responsible for the rheological behavior of the CMC solutions [9]. These entanglements are continuously and simultaneously destroyed and reformed when the shear rate was varied [8]. Thus, the critical concentration,  $c^{**}$ , which delimitates two different states of the polymer solution, semidiluted entangled network and concentrated solution [17], could be considered as the critical concentration at which the viscoelastic proprieties do appear in the polymer solutions.

## Conclusion

Different experimental measurements were carried out to assess in a reproducible and quantitative manner the rheological behavior of sodium CMC, a flexible anionic polymer. Using a controlled stress rheometer, the flow curves and dynamic properties were measured. It was found that no yield stress was observed for the aqueous solutions of CMC. The experimental results were found to be well correlated by the Cross model. The Cross parameters, i.e., zero shear rate viscosity,  $\mu_0$ , and reciprocal of the time constant,  $1/\lambda_c$ , allowed the determination of the critical concentration  $c^*$  and  $c^{**}$ . The creep and dynamic tests showed that CMC solutions exhibit concentration-dependent viscoelastic properties, with a dominant viscous behavior at CMC concentrations lower than  $c^{**}$  and a dominant elastic behavior at CMC concentrations higher than  $c^{**}$ . Furthermore, the measurement of the area of hysteresis loops resulting from upward–downward flow curves have shown

that the CMC solutions exhibit strong thixotropic behavior, more pronounced at the highest CMC concentrations.

**Acknowledgement** The authors would like to acknowledge the technical assistance of J. Monbled.

## References

1. Coussot P, Bertrand F, Herzhaft B (2004) *Oil Gas Sci Technol* 59:23
2. Benchabane A (2006) Doctorate Thesis (in French), ULP Strasbourg I, pp. 169
3. Benchabane A, Bekkour K (2006) *Rheol Acta* 45:425
4. Heinz A, Stengele RH, Plötze M (2004) *Annu Trans Nord Rheol Soc* 12:221
5. Amorim LV, Barbosa MIR, Lira H-L, Ferreira HC (2007) *Mat Res* 10:53
6. Dolz M, Jiménez J, Hernandez MJ, Delegido J, Casanovas A (2007) *J Petrol Sci Eng* 57:294
7. Ghannam MT, Esmail MN (1997) *J Appl Polym Sci* 64:289
8. Edali M, Esmail MN, Vatisas GH (2001) *J Appl Polym Sci* 79:1787
9. Kulicke W-M, Kull AH, Kull W, Thielking H, Engelhardt J, Pannek J-B (1996) *Polymer* 37:2723
10. Clasen C, Kulicke W-M (2001) *Prog Polym Sci* 26:1839
11. Barba C, Montané D, Farriol X, Desbrières J, Rinaudo M (2002) *Cellulose* 9:327
12. Escudier MP, Gouldson IW, Pereira AS, Pinho FT, Poole RJ (2001) *J Non-Newt Fluid Mech* 97:99
13. Renaud M, Belgacem MN, Rinaudo M (2005) *Polymer* 46:12348
14. Liu W-H, Yu TL, Lin H-L (2007) *Polymer* 48:4152
15. Dunstan DE, Hill EK, Wei Y (2004) *Polymer* 45:1261
16. Graessley WW (1980) *Polymer* 21:258
17. Grigorescu G, Kulicke W-M (2000) *Adv Polym Sci* 152:1
18. Bekkour K, Leyama M, Benchabane A, Scrivener O (2005) *J Rheol* 49:1329
19. Barnes HA (1997) *J Non-Newt Fluid Mech* 70:1
20. Mao C-F, Chen J-C (2006) *Food Hydrocolloids* 20:730
21. Lizarraga MS, Pianté Vicin DD, Gonzalez R, Rubiolo A, Santiago LG (2006) *Food Hydrocolloids* 20:740
22. Morris ER (1990) *Carbohydr Polym* 13:85
23. Manoj P, Watson AD, Hibberd DJ, Fillery-Travis AJ, Robins MM (1998) *J Colloid Interface Sci* 207:294
24. Inokuchi K (1955) *Bull Chem Soc Jpn* 20:453
25. Warburton B, Barry BW (1968) *J Pharm Pharmacol* 20:255
26. Duran JDG, Ramos-Tejada MM, Arroyo FJ, Gonzalez-Caballero F (2000) *J Colloid Interface Sci* 229:107